

# CHARACTERISTICS OF NATURAL RADIONUCLIDES AND $^{137}\text{Cs}$ IN SURFACE SOIL IN PHONSAVAN, XIENKHOANG, LAOS

by

**Thi-Hong BUI**<sup>1</sup>, **Van-Loat BUI**<sup>1\*</sup>, **Somsavath LEUANGTAKOUN**<sup>2</sup>,  
**Lemthong LATHDAVONG**<sup>2</sup>, **Sonexay XAYHUANGSY**<sup>2</sup>, **Duc-Thang DUONG**<sup>3</sup>,  
**Dinh-Khoa TRAN**<sup>4</sup>, **Van-Khanh TRAN**<sup>1</sup>, **Ngoc-Thiem LE**<sup>3</sup>, **Giang T. T. PHAN**<sup>5,6</sup>,  
**Van-Khanh HOANG**<sup>7\*</sup>, and **Hoai-Nam TRAN**<sup>7\*</sup>

<sup>1</sup>Faculty of Physics, VNU University of Science, Hanoi, Vietnam

<sup>2</sup>Department of Physics, Faculty of Natural Science, National University of Laos, Dongdok Vientiane, Laos

<sup>3</sup>Institute for Nuclear Science and Technology, Vietnam Atomic Energy Institute, Hanoi, Vietnam

<sup>4</sup>Dalat Nuclear Research Institute, Vietnam Atomic Energy Institute, Lamdong, Vietnam

<sup>5</sup>Institute of Fundamental and Applied Sciences, Duy Tan University, Da Nang, Vietnam

<sup>6</sup>Faculty of Natural Sciences, Duy Tan University, Da Nang, Vietnam

<sup>7</sup>Phenikaa Institute for Advanced Study, Phenikaa University, Hanoi, Vietnam

Scientific paper

<https://doi.org/10.2298/NTRP2304289B>

Assessment of the characteristics of natural radionuclides and  $^{137}\text{Cs}$  in soil in Phonsavan district, Xiengkhouang province, Laos has been conducted using a standard electrode coaxial Ge (SEGe) detector. Soil samples were collected at 20 locations close to the populated and agricultural area in Phonsavan district. The average activity concentrations of  $^{226}\text{Ra}$ ,  $^{238}\text{U}$ ,  $^{232}\text{Th}$ ,  $^{40}\text{K}$  and  $^{137}\text{Cs}$  are  $54.0 \pm 2.5$ ,  $65.1 \pm 4.4$ ,  $96.9 \pm 3.7$ ,  $433.2 \pm 20.7$ , and  $1.54 \pm 0.13 \text{ Bqkg}^{-1}$ , respectively. The average radium equivalent activity  $\text{Ra}_{\text{eq}}$  is  $225.9 \pm 7.8 \text{ Bqkg}^{-1}$ . The highest  $\text{Ra}_{\text{eq}}$  of  $269.9 \text{ Bqkg}^{-1}$  is still lower than the safety limit of  $370 \text{ Bqkg}^{-1}$ . Associated radiological hazard indices, such as absorbed gamma dose rate, outdoor annual effective dose equivalent, excess lifetime cancer risk, external and internal hazard indices, and gamma index, were also calculated and presented.

*Key words:* natural radionuclide,  $^{137}\text{Cs}$ , soil sample, activity concentration

## INTRODUCTION

The natural radionuclides including  $^{238}\text{U}$ ,  $^{232}\text{Th}$ , and  $^{40}\text{K}$  and their decay series in surface soils are the main contributors to the natural terrestrial gamma exposure [1, 2]. The  $^{238}\text{U}$  decay series is also referred to as  $^{226}\text{Ra}$  series since the  $^{226}\text{Ra}$  subseries accounts for about 98.5 % of the total gamma dose [3]. According to UNSCEAR report, the world average activity concentrations of  $^{226}\text{Ra}$ ,  $^{232}\text{Th}$ , and  $^{40}\text{K}$  in soils are 35, 30, and 400  $\text{Bqkg}^{-1}$ , respectively [1]. Soil is also the source for transferring radionuclides to plants [4-8]. Assessment in the activity concentrations of the natural radionuclides in soils is important in order to evaluate the radiological hazards to human health and for environmental protection and monitoring. Many studies have reported of the natural radionuclides in surface soil with different geological formations [9-17]. Besides the natural radionuclides, artificial radionuclides are being paid increasing attention as indicators to study environmental processes [18-21]. The  $^{137}\text{Cs}$  contamination in the

environment and soil originates from nuclear weapon tests and nuclear accidents in the past, *e. g.*, the Chernobyl and Fukushima disasters. Due to the chemical affinity for clay particles and organic matter,  $^{137}\text{Cs}$  is concentrated in the surface soil [2, 22]. The migration and dispersion of  $^{137}\text{Cs}$  are related to atmospheric circulation and fallout [23, 24]. Due to the atmospheric circulation and the fallout process, the  $^{137}\text{Cs}$  concentration is higher in the mountains. As a result of the erosion and washout flow,  $^{137}\text{Cs}$  is carried from the mountain to the surrounding foothills, making the activity concentrations of  $^{137}\text{Cs}$  at the foothills higher than other flat regions. Moreover, in a primitive forest, the amount of organic components in soil would be higher than in the other populated regions. The correlation between the  $^{137}\text{Cs}$  and organic components is higher, and thus, the  $^{137}\text{Cs}$  activity concentration is higher. The activity concentration of  $^{137}\text{Cs}$  depends on soil properties, biological disturbance, decay, mechanical removal with rainwater, vertical migration, and diffusion into deeper soil layers [23, 24]. Assessing the  $^{137}\text{Cs}$  radioactive contamination in soils is helpful to assess the characteristics, distribution, and relationship of  $^{137}\text{Cs}$  with geology, chemical properties, and the impact on the environmental ecology.

\* Corresponding authors, e-mail: buivanloat@hus.edu.vn  
khanh.hoangvan@phenikaa-uni.edu.vn  
nam.tranhoai@phenikaa-uni.edu.vn

In recent years, several studies have been conducted to assess the natural radionuclides in soils and to build up a baseline data in the middle of Laos for environmental protection and monitoring [25-28]. A previous work investigated the characteristics and distribution of  $^{137}\text{Cs}$  in soils in the middle of Laos [29]. The work aimed at providing the baseline data on the  $^{137}\text{Cs}$  for further monitoring. Among 212 soil samples collected evenly at the flat terrain with less variation in the petrographic properties, geology, and geological formations, the  $^{137}\text{Cs}$  activity was detected in 116 samples. The  $^{137}\text{Cs}$  activity concentrations were in the range of  $0.50\text{-}7.97\text{ Bqkg}^{-1}$  with the average value of  $1.46\text{ Bqkg}^{-1}$ . Preliminary relationship with geological formations, topographical factors and regional geology was discussed in [29]. A strong correlation between the natural radionuclides was observed, but almost no correlation between  $^{137}\text{Cs}$  and other parameters [29].

Xiangkhouang is a northern province of Laos, belonging to the Xiangkhouang plateau with the elevation of about 1300 m. Phonsavan district is the capital of the province having the average elevation of 1100 m, and is a potential region to examine the contamination of  $^{137}\text{Cs}$  in surface soil and the effect of the erosion and washout flow from the mountain. In the continuation of building up the baseline data of natural radionuclides and  $^{137}\text{Cs}$  in surface soil in Laos, the present work aimed at assessing the characteristics of natural radionuclides and  $^{137}\text{Cs}$  in Phonsavan district, Xiangkhouang province using the SEGe detector.

## MATERIALS AND METHODS

### Sampling sites and sample collection

Laos is a landlocked country in Southeast Asia, located on the latitude of  $14.117\text{-}23.684^\circ\text{N}$  and the longitude of  $100.413^\circ\text{-}108.832^\circ\text{E}$ . Xiangkhouang is a north-eastern province of the country on the Xiangkhouang

plateau, covering the area of  $15880\text{ km}^2$  with a largely mountainous topography. Xiangkhouang shares the borders with Luang Prabang and Houaphanh to the north, northern Vietnam to the east, Bolikhamxay and Vientiane to the south. Xiangkhouang is a part of Nam Ngum River watershed. The Xiangkhouang plateau is characterized by rolling hills and grassland with the elevation of about 1300 m. The highest peak is PhouBia (2820 m) in the southern part of the plateau. Phonsavan is the capital of Xiangkhouang province, located at the coordinates of  $19^\circ25'\text{N}$  and  $103^\circ10'\text{E}$  with a population of 37500. The city has a long, warm and wet summer and a short and dry winter. The climate is humid subtropical tempered by the average elevation of 1100 m. The average temperature in the summer is  $23.6^\circ\text{C}$ , and that in the winter is  $14.8^\circ\text{C}$ .

Soils were collected at 20 sampling sites close to the populated and agricultural area in Phonsavan district. Figure 1 displays the site map with the sampling locations. The samples were collected during the dry season in 2022. At each sampling site, the soil was collected from the surface layer with the depth of 0-30 cm. A square of 60 cm times 60 cm was determined and flattened. Top soils at the center and the corners of the square were collected and mixed up. The amount of 1 kg was selected based on a quarterly method. At the laboratory, after removing pieces of stones and large-size materials, the soils were dried in an oven at  $110^\circ\text{C}$  for 10-24 hours to remove the moisture content. Then, a sample of 180 g was weighed and packed in a standard plastic container (3.1 cm in height and 7.5 cm in diameter). The soil samples were stored for a month for attaining secular equilibrium between  $^{226}\text{Ra}$  and its daughters ( $^{214}\text{Bi}$  and  $^{214}\text{Pb}$ ).

### Detector calibration

The gamma spectra of the soil samples were measured using the Canberra spectrometer system with a

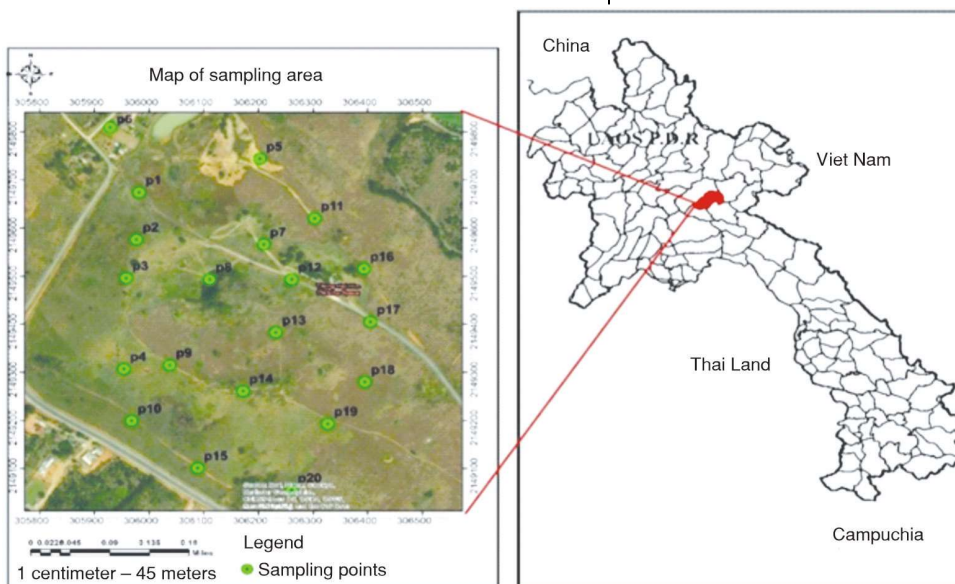


**Figure 1. Map of the sampling site in Phonsavan district, Xiangkhouang province, Laos with the locations of soil samples**

Standard Electrode Coaxial Ge (SEGe) detector (model GC 5019). The SEGe detector has the relative efficiency of 50 %, with the energy resolution of 1.9 keV at the 1332 keV peak of  $^{60}\text{Co}$  and the peak to Compton ratio (P/C) greater than 64. The detector is shielded in a chamber model 747. The gamma spectra measured by the SEGe detector were analyzed using the Genie 2000 software. Detector calibration was performed for determining the efficiency curve based on the measurement of the IAEA-375 reference material. In the measurement, the samples were placed on the top of the detector. The measurement time was increased to ensure the statistical errors (2) of important peaks are less than 2 %. In particular, the IAEA-375 reference material was measured for 100000 seconds. Background measurement was also conducted for the period of 160000 seconds. The detector's deadtime is less than 1 %. The efficiency curve of the SEGe detector was constructed based on the efficiency at the following peaks: 46.5 keV of  $^{210}\text{Pb}$ ; 63.3 keV of  $^{232}\text{Th}$ ; 186.2 keV of  $^{226}\text{Ra}$ ; 295.22 keV and 351.93 keV of  $^{214}\text{Pb}$ ; 609.31 keV, 1120.29 keV and 1764.49 keV of  $^{214}\text{Bi}$ ; 1460 keV of  $^{40}\text{K}$ . Figure 2 shows the efficiency curve of the SEGe detector with the gamma ray energy.

In environmental samples, the peak of 1460.83 keV of  $^{40}\text{K}$  is always disturbed by the peak of 1459.14 keV (0.87 %) of  $^{228}\text{Ac}$ . In the present work, the contribution of 1459.138 keV peak of  $^{228}\text{Ac}$  to the 1460.8 keV peak of  $^{40}\text{K}$  has been corrected by measuring the IAEA RTh1 reference material. During the sample counting process, in addition to the 1459.14 keV peak, the 911 keV (27.7 %) peak of  $^{228}\text{Ac}$  was also observed. The ratio between the count numbers of the 1459.14 keV and 911.1 keV peaks was determined and used to correct the contribution of  $^{232}\text{Th}$  (1459.14 keV) counts to the 1460.83 keV peak of  $^{40}\text{K}$ . By multiplying the counts of the 911 keV peak to the ratio, the counts of the 1459.14 keV peak is obtained to be subtracted. This subtraction eliminates the interference caused by  $^{228}\text{Ac}$  in the  $^{40}\text{K}$  region counts. The ratio be-

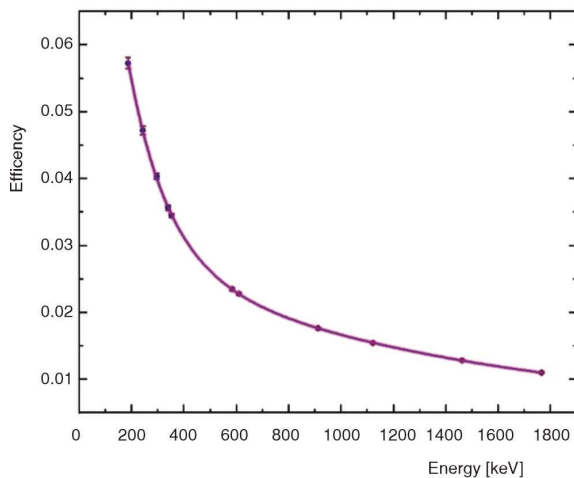


Figure 2. Efficiency curve of the SEGe detector as a function of gamma ray energy

tween the count numbers of the 1459.14 keV peak and the 911 keV peak is 0.0204.

### Radioactivity measurement

The measurement of the activity concentrations of  $^{226}\text{Ra}$ ,  $^{228}\text{Ac}$  ( $^{232}\text{Th}$ ),  $^{40}\text{K}$  and  $^{137}\text{Cs}$  were described in several previous works [26, 27, 29]. In particular, the  $^{226}\text{Ra}$  activity concentration was determined via the 295.57 keV (branching ratio of 0.1841) and 351.9 keV (0.3560) peaks of  $^{214}\text{Pb}$ , and the 609.3 keV (0.4549) and 1120.3 keV (0.1491) peaks of  $^{214}\text{Bi}$ .  $^{232}\text{Th}$  activity concentration was determined via the 338.6 keV (0.1127) and 911.1 keV (0.258) peaks of  $^{228}\text{Ac}$  and the 583.19 keV (0.3055) peak of  $^{208}\text{Tl}$ .  $^{40}\text{K}$  activity concentration was determined via the 1460 keV (0.1066) peak, and  $^{137}\text{Cs}$  activity concentration was evaluated via the 661.65 keV (0.851) peak. The activity concentration,  $A_X$  ( $\text{Bqkg}^{-1}$ ), of a radionuclide  $X$  is written as [30]

$$A_X = \frac{n(E_\gamma, X)}{\epsilon(E_\gamma) \cdot I(E_\gamma, X) \cdot m} \quad (1)$$

where  $n(E_\gamma, X)$  is the net counting rate (cps) for a peak at the energy  $E_\gamma$ ,  $\epsilon(E_\gamma)$  – the detector efficiency at the energy  $E_\gamma$ , and  $I(E_\gamma, X)$  – the gamma emission probability;  $m$  – the mass of soil sample. The  $2\sigma$  standard uncertainties are evaluated based on the uncertainties of the quantities in eq. (1). The minimum detectable activity (MDA) concentration of a radionuclide is

$$MDA_X = \frac{2.77 + 4.66\sqrt{N_B}}{\epsilon(E_\gamma) \cdot I(E_\gamma, X) \cdot m \cdot t} \quad (2)$$

where  $N_B$  is the background count for a peak at energy  $E_\gamma$ , and  $t$  – the measuring time. The MDA of  $^{137}\text{Cs}$  is 0.33  $\text{Bqkg}^{-1}$  with the measurement time of 24 hours following the method described in [29].

### Measurement of $^{238}\text{U}$

Several approaches are applicable to measure the  $^{238}\text{U}$  activity concentration in soil samples in the disequilibrium condition between  $^{226}\text{Ra}$  and  $^{238}\text{U}$ . In the disequilibrium between  $^{238}\text{U}$  and  $^{226}\text{Ra}$ , the activity concentration of  $^{238}\text{U}$  can be determined based on the gamma lines of its two first daughters in the decay series, *i. e.*,  $^{234}\text{Th}$  and  $^{234\text{m}}\text{Pa}$ , which are in equilibrium with  $^{238}\text{U}$ . In the first approach, the activity concentration of  $^{238}\text{U}$  can be determined via the 92.5 keV peak of  $^{234}\text{Th}$ . In this case, it needs to correct on the measurement for the self-absorption factors [31-33]. The second approach is to measure the  $^{238}\text{U}$  activity concentration via the 1001.03 keV peak of  $^{234\text{m}}\text{Pa}$ . Previous works indicated that the activity concentration of  $^{238}\text{U}$  could be determined based on the 1001.03 keV peak of  $^{234\text{m}}\text{Pa}$  without self-absorption correction [33, 34].

However, this measurement is applicable only in the case that the  $^{238}\text{U}$  activity concentration in soil sample is high enough or the measurement time is long enough. So that, the 1001.03 keV peak of  $^{234\text{m}}\text{Pa}$  appears clearly and isolated in the measured gamma spectrum [34]. The disadvantage of this approach is that if the activity concentration of  $^{238}\text{U}$  is not high enough, or the measurement time is not long enough, the count number of the 1001.03 keV peak is small, leading to a large statistical error.

Another approach is to measure the activity concentration of  $^{238}\text{U}$  based on the assumption that the atomic ratio of the two isotopes  $^{235}\text{U}$  and  $^{238}\text{U}$  ( $F = \frac{^{235}\text{U}}{^{238}\text{U}}$ ) is a constant, *i. e.*,  $F = 7.2 \cdot 10^{-3}$ . Based on the half-lives and the atomic masses of  $^{235}\text{U}$  and  $^{238}\text{U}$ , the ratio  $F_A$  of their activity concentrations is determined as

$$F_A = \frac{A_{^{235}\text{U}}}{A_{^{238}\text{U}}} = 0.0462 \quad (3)$$

The activity concentration of  $^{235}\text{U}$  is determined from its 185.72 keV (0.572) peak. Since the 185.71 keV peak of  $^{235}\text{U}$  and the 186.21 keV peak of  $^{226}\text{Ra}$  were overlapped, forming a total peak of 186 keV. The count rate of the total 186 keV peak is the sum of the two peaks and can be expressed as

$$n(186) = n(185.75, ^{235}\text{U}) + n(186.21, ^{226}\text{Ra}) \quad (4)$$

where  $n(186)$  is the count rate (cps) of the total 186 keV peak, and  $n(185.75, ^{235}\text{U})$  and  $n(186.21, ^{226}\text{Ra})$  are the count rates due to the 185.71 keV peak of  $^{235}\text{U}$  and the 186.21 keV peak of  $^{226}\text{Ra}$ , respectively. In the equilibrium condition between  $^{226}\text{Ra}$  and  $^{214}\text{Pb}$ , the activity concentration of  $^{226}\text{Ra}$  is calculated as

$$A_{^{226}\text{Ra}} = \frac{n(186.21, ^{226}\text{Ra})}{\epsilon(186.21) \cdot I(186.21, ^{226}\text{Ra}) \cdot m} \quad (5)$$

where

$$n(186.21, ^{226}\text{Ra}) = \frac{\epsilon(186.21) \cdot I(186.21, ^{226}\text{Ra})}{\epsilon(295.22) \cdot I(295.22, ^{214}\text{Pb}) \cdot n(295.22, ^{214}\text{Pb})} \quad (6)$$

where  $I(E_\gamma, X)$  is the emission probability for the gamma-ray at energy  $E_\gamma$ , and  $\epsilon(E_\gamma)$  – the detection efficiency. From eqs. (4) and (6), the count rate  $n(185.75, ^{235}\text{U})$  is determined as

$$n(185.75, ^{235}\text{U}) = n(186) - \frac{\epsilon(186.21) \cdot I(186.21, ^{226}\text{Ra})}{\epsilon(295.22) \cdot I(295.22, ^{214}\text{Pb}) \cdot n(295.22, ^{214}\text{Pb})} \quad (7)$$

Once the count rate  $n(185.75, ^{235}\text{U})$  is known, the activity concentration of  $^{235}\text{U}$  can be obtained from eq. (4). In the present work, the activity concentrations of  $^{238}\text{U}$  in soil samples were measured based on both the 1001.03 keV peak and the activity concentration of  $^{235}\text{U}$  using the SEGe detector. The measurements were conducted based on a secondary reference material TNUKTh, which was developed by a mixture of the IAEA reference materials. The compositions of the TNUKTh secondary reference material consist of RGU-1 ( $12.00 \pm 0.01$  g), RGTh<sup>-1</sup> ( $12.00 \pm 0.01$  g), RGK-1 ( $13.50 \pm 0.01$  g), SiO<sub>2</sub> ( $57.00 \pm 0.01$  g), CaCO<sub>3</sub> ( $57.00 \pm 0.01$  g), MgO ( $18.00 \pm 0.01$  g), TiO<sub>2</sub> ( $9.00 \pm 0.01$  g) and Ba(NO<sub>3</sub>)<sub>2</sub> ( $57.00 \pm 0.01$  g). The gamma spectrum of the TNUKTh secondary reference material measured by the SEGe detector for a period of 90000 s is displayed in fig. 3. Table 1 shows the activity concentrations of  $^{238}\text{U}$ ,  $^{226}\text{Ra}$ ,  $^{232}\text{Th}$ , and  $^{40}\text{K}$  in the TNUKTh secondary reference material measured by the SEGe detector. Comparison with the reference values is also presented. The result shows that the activity concen-

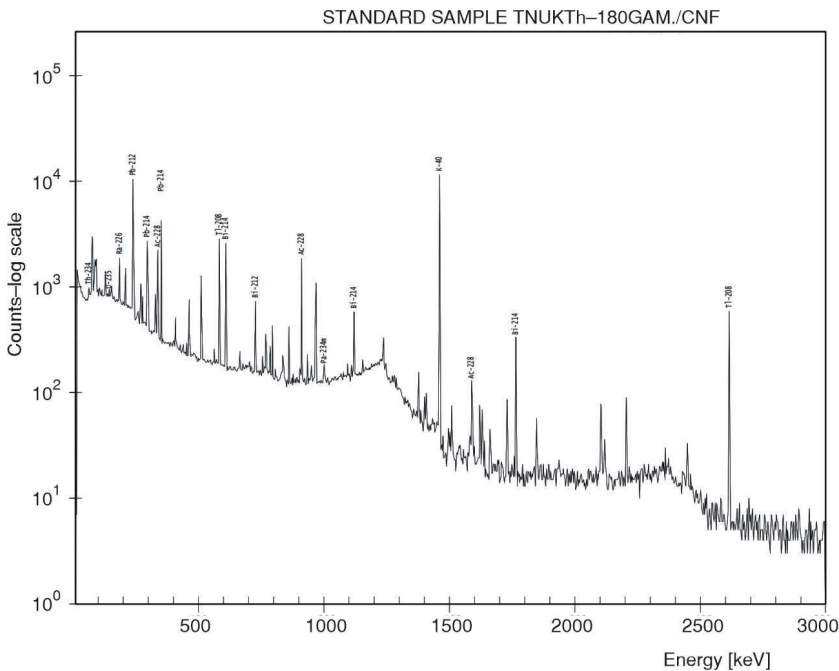


**Figure 3. Gamma ray spectrum of the TNUKTh secondary reference material measured by the SEGe detector**

**Table 1. Activity concentrations of <sup>238</sup>U, <sup>232</sup>Th, <sup>40</sup>K, and <sup>137</sup>Cs of the TNUKTh secondary reference material measured by the SEGe detector**

Radionuclides	This measurement [Bqkg <sup>-1</sup> ]	Reference [Bqkg <sup>-1</sup> ]	Difference [%]
<sup>238</sup> U (1001.03 keV)	315.8 ±12.1	334.5 ±6.7	-5.59
<sup>238</sup> U ( <sup>235</sup> U)	339.7 ±12.5	334.5 ±6.7	1.55
<sup>226</sup> Ra	331.5 ±6.7	334.5 ±6.7	-0.97
<sup>232</sup> Th	225.4 ±9.1	216.7 ±11.0	4.01
<sup>40</sup> K	958.5 ±33.2	972.2 ±11.2	-1.41

tration of <sup>238</sup>U measured via the 1001.03 keV peak is underestimated by -5.59% compared to the reference value. Whereas, that measured by the activity concentration of <sup>235</sup>U is greater than the reference value by 1.55%. The differences in the activity concentrations of the natural radionuclides are within 5.59%, which is acceptable for further measurement of the soil samples.

It is noticed that in addition to the 185.75 keV (57.2%) peak, <sup>235</sup>U can also be directly determined based on the 143.76 keV (10.96%), 163.35 keV (5.08%) and 205.30 (5.08%) peaks. However, since the soil samples were measured using the wide-band gamma spectrometer system from 30 keV to 3.0 MeV, the photoelectric absorption peaks of <sup>235</sup>U were emitted, including the 143.76 keV peak, and thus Compton scattering is high. In contrast, the 1001.03 keV peak of <sup>234m</sup>Pa appears clearly against the low Compton scattering background, fig. 3. The statistical error of the count rate of the 143.76 keV peak (12%) is greater than that of the 1001.03 keV peak (6.8%). Therefore, the determination of <sup>235</sup>U based on the 143.76 keV peak would affect the accuracy of the activity concentration of <sup>238</sup>U. Table 1 shows that the determination of the <sup>235</sup>U based on the 185.75 keV peak infers the radioactive activity of <sup>238</sup>U with a high accuracy (discrepancy less than <2%).

### Radiological hazards

To estimate the impact of the natural radionuclides to human health, radiological hazard indices were calculated, including radium equivalent activity,  $Ra_{eq}$ , absorbed gamma dose rate,  $D$ , outdoor annual effective dose equivalent (AEDE), excess lifetime cancer risk (ELCR), external and internal hazard indices ( $H_{ex}$  and  $H_{in}$ ), and radioactivity level index  $I_\gamma$ . The  $Ra_{eq}$  is calculated as follows [35, 36]

$$Ra_{eq} = A_{Ra} + 1.43A_{Th} + 0.077A_K \quad (8)$$

where  $A_{Ra}$ ,  $A_{Th}$ , and  $A_K$  are the activity concentrations of <sup>226</sup>Ra, <sup>232</sup>Th, and <sup>40</sup>K, respectively. The absorbed gamma dose rate  $D$  (nGyh<sup>-1</sup>) at 1 m above the ground is calculated as [1]

$$D(\text{nGyh}^{-1}) = 0.46A_{Ra} + 0.62A_{Th} + 0.042A_K \quad (9)$$

where the conversion factors associated to <sup>226</sup>Ra, <sup>232</sup>Th, and <sup>40</sup>K are 0.46, 0.62, and 0.042 nGyh<sup>-1</sup>/(Bqkg<sup>-1</sup>), respectively. The outdoor AEDE (mSv per year) is calculated as [1]

$$AEDE(\text{mSv per year}) = D \cdot DCF \cdot OF \cdot T \quad (10)$$

where the absorbed gamma dose rate  $D$  (nGyh<sup>-1</sup>) is obtained from eq. (3),  $DCF = 0.7 \text{ SvGy}^{-1}$  – the dose conversion factor,  $OF = 0.2$  – the outdoor occupancy factor, and  $T = 8760 \text{ h}$  – the time factor [1, 37]. From the outdoor annual effective dose equivalent AEDE, the excess lifetime cancer risk (ELCR) is calculated as follows [38]

$$ELCR = AEDE \cdot DL \cdot RF \quad (11)$$

where  $DL$  and  $RF$  are the duration of life (70 years average) and the risk factor (Sv<sup>-1</sup>), respectively. For the public, the value of  $RF = 0.05 \text{ Sv}^{-1}$  was used according to ICRP [39]. The external and internal hazard indices,  $H_{ex}$  and  $H_{in}$ , are calculated as [36, 40]

$$H_{ex} = \frac{A_{Ra}}{370} + \frac{A_{Th}}{259} + \frac{A_K}{4810} \quad (12)$$

$$H_{in} = \frac{A_{Ra}}{185} + \frac{A_{Th}}{259} + \frac{A_K}{4810} \quad (13)$$

The radiological hazard associated with the natural radionuclides can also be evaluated via the gamma index  $I_\gamma$ , which is calculated as

$$I_\gamma = \frac{A_{Ra}}{300} + \frac{A_{Th}}{200} + \frac{A_K}{3000} \quad (14)$$

The value of  $I_\gamma = 1.0$  is equivalent to the effective radiation dose of 1 mSvy<sup>-1</sup>, which is used as the upper limit.

## RESULTS AND DISCUSSION

### Activity concentrations of the radionuclides

Table 2 presents the activity concentrations of <sup>226</sup>Ra, <sup>238</sup>U, <sup>232</sup>Th, <sup>40</sup>K, and <sup>137</sup>Cs in 20 soil samples in Phonsavan district. The <sup>226</sup>Ra activity concentration varies in the range of 41.7-72.1 Bqkg<sup>-1</sup> with the average value of 54.0 ±2.5 Bqkg<sup>-1</sup>. The activity concentration of <sup>238</sup>U is 40.9-84.5 Bqkg<sup>-1</sup> with the average value of 65.1 ±4.4 Bqkg<sup>-1</sup>. The highest <sup>226</sup>Ra and <sup>238</sup>U activity concentrations are observed at the sample S10. The <sup>232</sup>Th activity concentrations in 20 soil samples are within the range of 69.8-125.7 Bqkg<sup>-1</sup>. The highest value of 125.7 ±4.8 Bqkg<sup>-1</sup> is found at the sample S20. Sample S15 corresponds to the lowest <sup>232</sup>Th activity concentration. The average value is 96.9 ±3.7 Bqkg<sup>-1</sup>. The activity concentrations of <sup>40</sup>K vary from 147.2 to 829.1 Bqkg<sup>-1</sup>, with the average value of 433.2 ±20.7 Bqkg<sup>-1</sup>. The highest <sup>40</sup>K activity concentration of 829.1 ±36.1 Bqkg<sup>-1</sup> is found at the sample S4. Table

**Table 2. Activity concentrations of radionuclides in soil samples in Phonsavan district**

Samples	Activity concentration [ $\text{Bqkg}^{-1}$ ]				
	$^{226}\text{Ra}$	$^{238}\text{U}$	$^{232}\text{Th}$	$^{40}\text{K}$	$^{137}\text{Cs}$
S1	56.3 ±2.6	71.5 ±4.7	108.1 ±4.6	609.3 ±27.4	2.35 ±0.17
S2	62.2 ±3.4	77.1 ±4.8	113.2 ±4.7	329.7 ±16.3	1.75 ±0.16
S3	56.7 ±2.6	72.5 ±4.7	106.5 ±4.3	770.5 ±34.7	–
S4	42.1 ±1.7	40.9 ±3.1	72.8 ±2.6	829.1 ±36.1	1.97 ±0.16
S5	47.0 ±1.7	62.0 ±4.3	85.5 ±3.0	357.2 ±15.3	1.92 ±0.16
S6	46.8 ±1.7	63.1 ±4.3	87.4 ±3.1	451.6 ±0.3	1.81 ±0.16
S7	52.2 ±2.4	69.7 ±4.8	92.6 ±3.6	147.2 ±8.2	3.12 ±0.20
S8	54.2 ±2.4	72.0 ±4.7	97.6 ±3.7	189.6 ±11.2	2.16 ±0.17
S9	57.6 ±2.7	75.4 ±4.8	113.4 ±4.7	291.3 ±15.5	1.54 ±0.14
S10	72.1 ±3.7	84.5 ±5.1	118.3 ±4.7	371.8 ±22.3	1.61 ±0.14
S11	69.0 ±3.5	82.1 ±5.0	108.1 ±4.3	426.3 ±20.4	1.79 ±0.15
S12	63.2 ±3.5	67.0 ±4.8	104.2 ±4.3	456.3 ±21.1	0.65 ±0.06
S13	56.4 ±2.7	78.9 ±4.8	96.7 ±3.7	256.3 ±15.1	1.73 ±0.15
S14	52.7 ±2.4	61.1 ±4.3	77.2 ±2.7	235.1 ±14.6	1.82 ±0.16
S15	45.9 ±1.8	46.9 ±3.8	69.8 ±2.6	336.2 ±15.1	1.30 ±0.12
S16	41.7 ±1.6	41.9 ±3.1	82.5 ±3.0	539.3 ±25.2	0.83 ±0.08
S17	53.5 ±2.4	63.7 ±4.4	97.9 ±3.2	337.8 ±15.1	1.85 ±0.16
S18	56.4 ±2.7	65.3 ±4.5	90.6 ±3.5	765.4 ±34.7	–
S19	46.2 ±1.8	47.7 ±3.8	89.2 ±3.1	448.4 ±21.0	1.35 ±0.12
S20	48.2 ±1.9	58.4 ±4.3	125.7 ±4.8	516.2 ±24.8	1.25 ±0.12
Min	41.7 ±1.6	40.9 ±3.1	69.8 ±2.6	147.2 ±8.2	0.65 ±0.06
Max	72.1 ±3.7	84.5 ±5.1	125.7 ±4.8	829.1 ±36.1	3.12 ±0.20
Average	54.0 ±2.5	65.1 ±4.4	96.9 ±3.7	433.2 ±20.7	1.54 ±0.13
SD	8.27	12.8	15.34	192.18	0.74
SE	1.85	2.86	3.43	42.97	0.17
Median	53.9	66.2	97.2	399.0	1.74
Skewness	0.54	–0.54	–0.01	0.71	–0.49
Kurtosis	–0.04	–0.47	–0.69	–0.13	0.98

**Table 3. Comparison of the activity concentrations of the natural radionuclides in Phonsavan with neighbouring regions**

Region	Activity concentration [ $\text{Bqkg}^{-1}$ ]				References
	$^{238}\text{U}$	$^{226}\text{Ra}$	$^{232}\text{Th}$	$^{40}\text{K}$	
Phonsavan, Xiengkhouang, Laos	54 <sup>a</sup> (41.7-72) <sup>b</sup>	65 (41-85)	97 (70-126)	433 (147-829)	This work
Savannakhet, Laos	–	22 (7-74)	31 (4-114)	212 (14-906)	[26]
Bolikhamxay, Laos	–	44 (13-90)	63 (11-93)	523 (38-999)	[27]
Khammuoan, Laos	–	22 (7-74)	31 (4-114)	212 (14-906)	[28]
Nghe An, Vietnam	–	55	75	438	[13]
Ha Tinh, Vietnam	–	45	63	488	[13]
Quang Binh, Vietnam	–	39	48	319	[13]
Ho Chi Minh, Vietnam	–	55	75	438	[16]
Southern Thailand	4-122	29 (4-122)	44 (6-170)	344 (5-1422)	[41]
Perak, Malaysia	12-426	112 (12-426)	246 (19-1377)	277 (19-2204)	[11]
Penang, Malaysia	184	<sup>396</sup> 162 (12-968)	165 (16-667)	835 (87-1827)	[42]
Johor, Malaysia	–	–	261 (11-1210)	300 (12-2450)	[43]
World average	–	32	45	412	[1]

<sup>a</sup> Average value and <sup>b</sup> range of the values

3 presents a comparison of the activity concentrations of the natural radionuclides in surface soils in Phonsavan district with that obtained in neighbouring regions. One can see that the activity concentrations of  $^{226}\text{Ra}$ ,  $^{232}\text{Th}$ , and  $^{40}\text{K}$  in Phonsavan district are higher than that obtained in the middle of Laos. The average

values in this study are also higher than the world average values [1]. Figure 4 displays the frequency distributions of the activity concentrations of the radionuclides. The symmetrical distributions are observed for all the natural radionuclides and  $^{137}\text{Cs}$  with approximate zero skewness. The concentrations of all

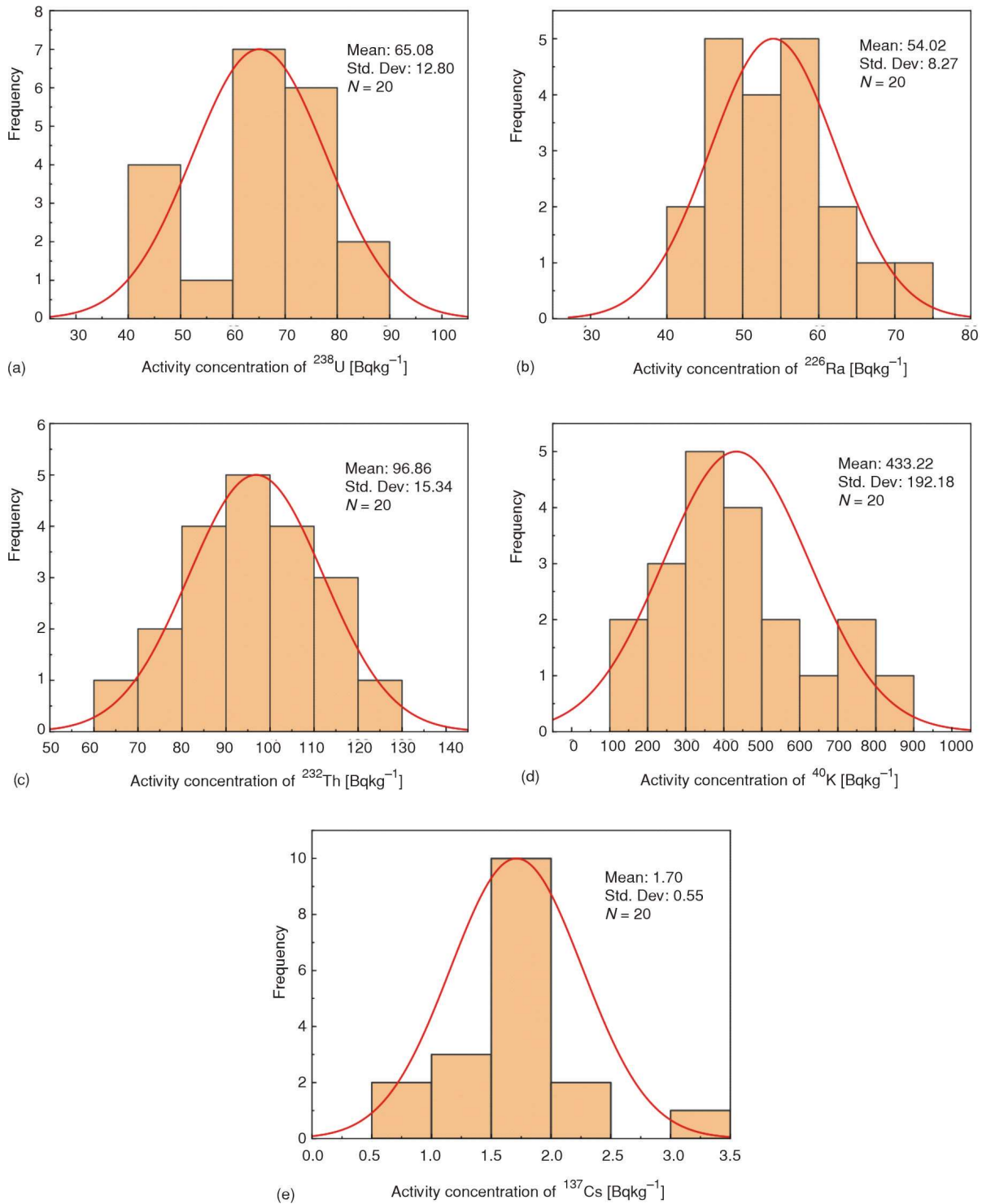


**Figure 4. Frequency distribution of the activity concentrations in the soil samples in Phonsavan district**

the radionuclides followed the light-tailed distribution with the Kurtosis ranging from  $-0.69$  to  $0.98$ . Figure 5 displays the Pearson correlation coefficients among the activity concentrations of the natural radionuclides and  $^{137}\text{Cs}$  obtained in Phonsavan district. Strong correlation is observed among  $^{226}\text{Ra}$ ,  $^{238}\text{U}$ , and  $^{232}\text{Th}$ . However, no correlation between  $^{40}\text{K}$  and  $^{137}\text{Cs}$  with others is observed.

As shown in tab. 2, among 20 soil samples collected, the  $^{137}\text{Cs}$  activity was detected in 18 samples. The  $^{137}\text{Cs}$  activity concentrations are about  $0.65\text{--}3.12\text{ Bqkg}^{-1}$  with the average value of  $1.54 \pm 0.13\text{ Bqkg}^{-1}$ . The highest value of  $3.12 \pm 0.20\text{ Bqkg}^{-1}$  was obtained at the sample S7. This result is consistent with the hypothesis that  $^{137}\text{Cs}$  is more concentrated in the foothills due to the erosion and washout flow from the mountain. Compared to the

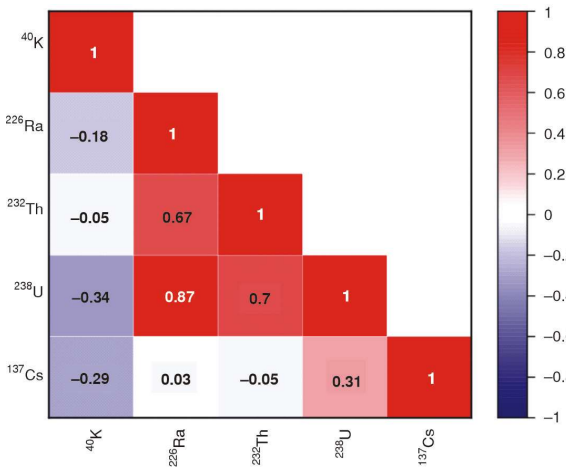


**Figure 5. Pearson correlation coefficients between the activity concentrations of the radionuclides in the soil samples in Phonsavan district**

concentration of  $^{137}\text{Cs}$  in the middle of Laos (average of  $1.42$  and range of  $0.5\text{--}7.97$   $\text{Bqkg}^{-1}$ ) [29], the values obtained in Phonsavan district are within this range. The  $^{137}\text{Cs}$  concentration in Phonsavan is lower than the world average value ( $51$   $\text{Bqkg}^{-1}$ ) [1].

## Radiological hazards

### Radium equivalent activity

Table 4 presents the radium equivalent activity  $\text{Ra}_{\text{eq}}$ , absorbed gamma dose rate  $D$ , outdoor annual effective dose equivalent AEDE and excess lifetime cancer risk ELCR, calculated from the activity concentrations of the radionuclides in 20 soil samples. Figure 6 displays the  $\text{Ra}_{\text{eq}}$  values with the contribution from the natural radionuclides. One can see that the  $\text{Ra}_{\text{eq}}$  values are within  $171.6\text{--}269.9$   $\text{Bqkg}^{-1}$ , with the average of  $225.9 \pm 7.8$   $\text{Bqkg}^{-1}$ , which is higher than the world average value by a factor of 2.0. The average  $\text{Ra}_{\text{eq}}$  in this study area is also higher than that obtained in the middle of Laos ( $121.8$   $\text{Bqkg}^{-1}$ ) by a factor of 1.9 [28]. The highest  $\text{Ra}_{\text{eq}}$  of  $269.9 \pm 9.1$   $\text{Bqkg}^{-1}$  is obtained at the sample S10. This value is still lower than the safety limit of  $370$   $\text{Bqkg}^{-1}$  [1]. The average contributions of  $^{226}\text{Ra}$ ,  $^{232}\text{Th}$ , and  $^{40}\text{K}$  to the total  $\text{Ra}_{\text{eq}}$  are 24.0, 61.3, and 14.7 %, respectively.

**Table 4. Radium equivalent activity concentration  $\text{Ra}_{\text{eq}}$ , absorbed gamma dose rate  $D$ , outdoor annual effective dose equivalent AEDE and effective life cancer risk ELCR in the soil samples in Phonsavan district**

Sample	$\text{Ra}_{\text{eq}}$ [ $\text{Bqkg}^{-1}$ ]	$D$ [ $\text{nGy}^{-1}$ ]	AEDE [ $\text{mSvy}^{-1}$ ]	ELCR [ $\times 10^{-3}$ ]
S1	$257.8 \pm 9.7$	$118.5 \pm 5.2$	$0.14 \pm 0.006$	$0.50 \pm 0.02$
S2	$249.5 \pm 8.0$	$112.7 \pm 5.2$	$0.14 \pm 0.006$	$0.48 \pm 0.02$
S3	$268.2 \pm 11.2$	$124.4 \pm 5.3$	$0.15 \pm 0.006$	$0.53 \pm 0.02$
S4	$210.0 \pm 10.6$	$99.3 \pm 3.9$	$0.12 \pm 0.005$	$0.42 \pm 0.02$
S5	$196.7 \pm 5.8$	$89.6 \pm 3.3$	$0.11 \pm 0.004$	$0.38 \pm 0.01$
S6	$206.5 \pm 7.0$	$94.7 \pm 3.6$	$0.11 \pm 0.004$	$0.40 \pm 0.02$
S7	$195.9 \pm 5.4$	$87.6 \pm 3.7$	$0.11 \pm 0.004$	$0.37 \pm 0.02$
S8	$208.4 \pm 6.0$	$93.4 \pm 3.9$	$0.11 \pm 0.005$	$0.39 \pm 0.02$
S9	$242.1 \pm 7.6$	$109.0 \pm 4.8$	$0.13 \pm 0.006$	$0.46 \pm 0.02$
S10	$269.9 \pm 9.1$	$122.1 \pm 5.5$	$0.15 \pm 0.007$	$0.52 \pm 0.02$
S11	$256.4 \pm 8.4$	$116.7 \pm 5.1$	$0.14 \pm 0.006$	$0.49 \pm 0.02$
S12	$247.4 \pm 8.5$	$112.9 \pm 5.2$	$0.14 \pm 0.006$	$0.48 \pm 0.02$
S13	$214.4 \pm 6.7$	$96.7 \pm 4.2$	$0.12 \pm 0.005$	$0.41 \pm 0.02$
S14	$181.2 \pm 5.7$	$82.0 \pm 3.4$	$0.10 \pm 0.004$	$0.35 \pm 0.01$
S15	$171.7 \pm 5.5$	$78.5 \pm 3.1$	$0.09 \pm 0.004$	$0.33 \pm 0.01$
S16	$201.2 \pm 8.0$	$93.0 \pm 3.7$	$0.11 \pm 0.004$	$0.39 \pm 0.02$
S17	$219.5 \pm 6.2$	$99.5 \pm 3.7$	$0.12 \pm 0.005$	$0.42 \pm 0.02$
S18	$244.9 \pm 10.8$	$114.3 \pm 4.9$	$0.14 \pm 0.006$	$0.48 \pm 0.02$
S19	$208.4 \pm 7.1$	$95.4 \pm 3.6$	$0.12 \pm 0.004$	$0.40 \pm 0.02$
S20	$267.7 \pm 9.2$	$121.8 \pm 4.9$	$0.15 \pm 0.006$	$0.51 \pm 0.02$
Min	$171.7 \pm 5.5$	$78.5 \pm 3.1$	$0.09 \pm 0.004$	$0.33 \pm 0.01$
Max	$269.9 \pm 9.1$	$124.4 \pm 5.3$	$0.15 \pm 0.007$	$0.53 \pm 0.02$
Average	$225.9 \pm 7.8$	$103.1 \pm 4.3$	$0.12 \pm 0.01$	$0.44 \pm 0.02$
SD	30.6	14.2	0.02	0.06
SE	6.84	3.16	0.004	0.02
Median	216.99	99.41	0.12	0.73
Skewness	-0.02	-0.02	-0.02	0.07
Kurtosis	-1.26	-1.25	-1.26	-1.35

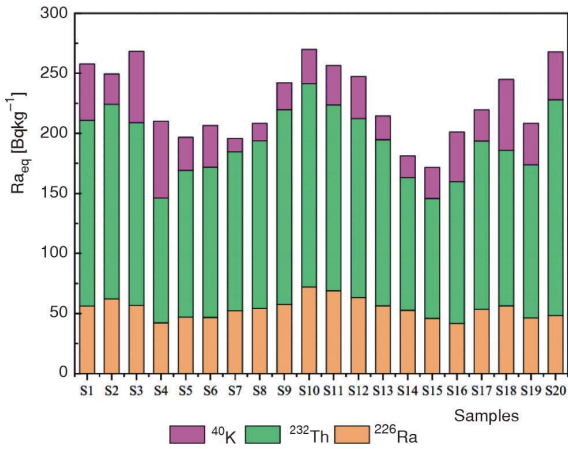


**Figure 6.** The  $Ra_{eq}$  in the soil samples in Phonsavan district

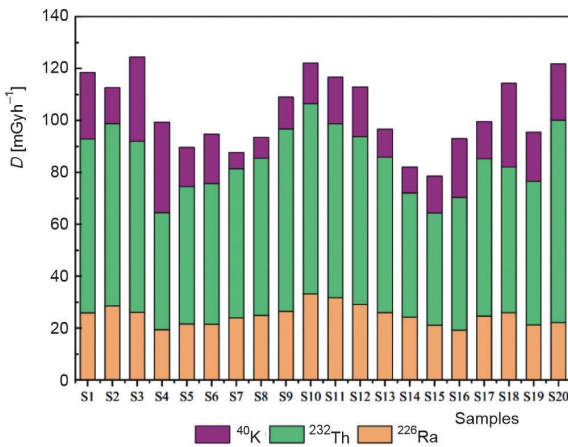


**Figure 7.** Absorbed gamma dose rate  $D$  in the soil samples in Phonsavan district

**Absorbed gamma dose rate**

The absorbed gamma dose rates  $D$  [ $\text{nGy}\cdot\text{h}^{-1}$ ] of the terrestrial gamma radiation were calculated in 20 soil samples in Phonsavan. The results show that  $D$  values are within the range of  $78.5\text{-}124.4$   $\text{nGy}\cdot\text{h}^{-1}$  as shown in tab. 4 and fig. 7. The highest  $D$  is  $124.4$   $\text{nGy}\cdot\text{h}^{-1}$ , and the average value is  $103.1 \pm 4.3$   $\text{nGy}\cdot\text{h}^{-1}$ . This value is about 1.38 times greater than the world average value as shown in tab. 3. It is estimated that the contributions of  $^{226}\text{Ra}$ ,  $^{232}\text{Th}$ , and  $^{40}\text{K}$  to the total dose rate are 24 %, 58 %, and 18 %, respectively.

**Annual effective dose equivalent and excess lifetime cancer risk**

The outdoor AEDE varies from 0.02 to 0.15  $\text{mSv}\cdot\text{y}^{-1}$  as shown in tab. 4. Figure 8 depicts the AEDE and the ECLR calculated from the soil samples in Phonsavan district. The contributions of  $^{226}\text{Ra}$ ,  $^{232}\text{Th}$ , and  $^{40}\text{K}$  to the total AEDE are estimated of about 25,

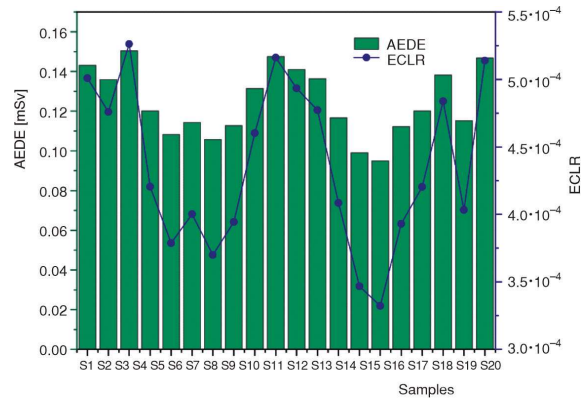


**Figure 8.** The AEDE (mSv) and the ECLR in the soil samples in Phonsavan district

48 and 27 %, respectively. The highest AEDE of  $0.15$   $\text{mSv}\cdot\text{y}^{-1}$  is obtained at the sample S10. The average AEDE is  $0.12$   $\text{mSv}\cdot\text{y}^{-1}$ . The values are smaller than the world average [1], and much lower than the safety limit of  $1.0$   $\text{mSv}\cdot\text{y}^{-1}$  [39]. From the AEDE, the ECLR values are obtained in the range from  $0.33\cdot 10^{-3}$  to  $0.53\cdot 10^{-3}$  with the average value of  $0.44\cdot 10^{-3}$  as shown in tab. 3. It is noticed that the ECLR in surface soil in Phonsavan is greater than the world average value of  $0.29\cdot 10^{-3}$ .

**External and internal radiological hazards and gamma index**

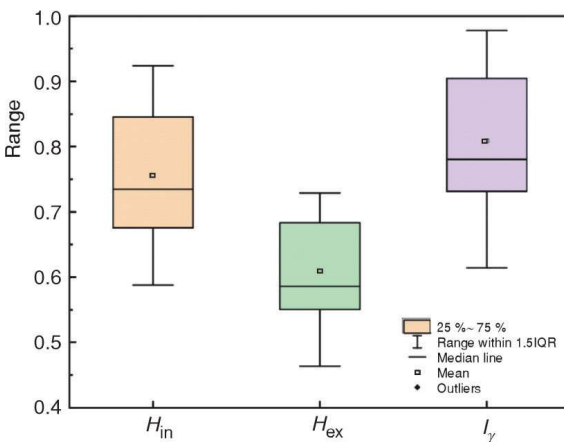
Table 5 shows the external and internal radiological hazards and the radioactivity level index calculated from the activity concentrations in the soil samples. Figure 9 depicts the statistical analysis of  $H_{ex}$ ,  $H_{in}$  and  $I_\gamma$ . The  $H_{ex}$  values are in the range of  $0.46\text{-}0.73$  with the average of  $0.61$ . The  $H_{in}$  is about  $0.59\text{-}0.92$  with the average of  $0.76$ . The contributions of  $^{226}\text{Ra}$ ,  $^{232}\text{Th}$ , and  $^{40}\text{K}$  to the  $H_{ex}$  are about 24, 61, and 15%, respectively, and that values to the  $H_{in}$  are 38, 49 and 12 %, respectively. It is noticed that the  $H_{ex}$  and  $H_{in}$  in the soils in Phonsavan are less than the safety limits (1.0). The  $I_\gamma$  varies in the range of  $0.61\text{-}0.98$  with the average value of  $0.81$ . The values are lower than the limit of 1.0.

**CONCLUSIONS**

Assessment on characteristics of natural radionuclides and  $^{137}\text{Cs}$  in surface soils in Phonsavan district, Xiengkhouang province, Laos have been conducted using the SEGe detector. Twenty soil samples were collected in the populated and agricultural area in Phonsavan district. The average activity concentrations of  $^{238}\text{U}$ ,  $^{226}\text{Ra}$ ,  $^{232}\text{Th}$ , and  $^{40}\text{K}$  are  $65.1 \pm 4.4$   $\text{Bqkg}^{-1}$ ,  $54.0 \pm 2.5$   $\text{Bqkg}^{-1}$ ,  $96.9 \pm 3.7$   $\text{Bqkg}^{-1}$ , and  $433.2 \pm 20.7$   $\text{Bqkg}^{-1}$ , respectively. The average  $Ra_{eq}$  is

**Table 5. Radiological hazard indices of  $H_{\text{ex}}$ ,  $H_{\text{in}}$ , and  $I_{\gamma}$  in the soil samples in Phonsavan district**

Sample	$H_{\text{ex}}$	$H_{\text{in}}$	$I_{\gamma}$
S1	0.70 ± 0.03	0.85 ± 0.04	0.93 ± 0.04
S2	0.67 ± 0.03	0.84 ± 0.04	0.88 ± 0.04
S3	0.72 ± 0.03	0.88 ± 0.04	0.98 ± 0.04
S4	0.57 ± 0.02	0.68 ± 0.03	0.78 ± 0.03
S5	0.53 ± 0.02	0.66 ± 0.02	0.40 ± 0.03
S6	0.56 ± 0.02	0.68 ± 0.03	0.74 ± 0.03
S7	0.53 ± 0.02	0.67 ± 0.03	0.69 ± 0.03
S8	0.56 ± 0.02	0.71 ± 0.03	0.73 ± 0.03
S9	0.65 ± 0.03	0.81 ± 0.04	0.86 ± 0.04
S10	0.73 ± 0.03	0.92 ± 0.04	0.96 ± 0.04
S11	0.69 ± 0.03	0.88 ± 0.04	0.91 ± 0.04
S12	0.67 ± 0.03	0.84 ± 0.04	0.88 ± 0.04
S13	0.58 ± 0.02	0.73 ± 0.03	0.76 ± 0.03
S14	0.49 ± 0.02	0.63 ± 0.03	0.64 ± 0.03
S15	0.46 ± 0.02	0.59 ± 0.02	0.61 ± 0.02
S16	0.54 ± 0.02	0.66 ± 0.03	0.73 ± 0.03
S17	0.59 ± 0.02	0.74 ± 0.03	0.78 ± 0.03
S18	0.66 ± 0.03	0.81 ± 0.04	0.90 ± 0.04
S19	0.56 ± 0.02	0.69 ± 0.03	0.75 ± 0.03
S20	0.72 ± 0.03	0.85 ± 0.03	0.96 ± 0.04
Min	0.46 ± 0.02	0.59 ± 0.02	0.61 ± 0.02
Max	0.73 ± 0.03	0.92 ± 0.04	0.98 ± 0.04
Average	0.61	0.76	0.81

**Figure 9. The  $H_{\text{ex}}$ ,  $H_{\text{in}}$ , and  $I_{\gamma}$  calculated from the soil samples in Phonsavan district**

225.9 ± 7.8 Bqkg<sup>-1</sup>. The contributions of  $^{226}\text{Ra}$ ,  $^{232}\text{Th}$ , and  $^{40}\text{K}$  in the  $Ra_{\text{eq}}$  are about 24.0 %, 61.3 %, and 14.7 %, respectively. The highest  $^{226}\text{Ra}$  of 269.9 ± 9.1 Bqkg<sup>-1</sup> obtained in Phonsavan is still lower than the safety limit of 370 Bqkg<sup>-1</sup>. Among 20 soil samples collected in Phonsavan district, the  $^{137}\text{Cs}$  activity were detected in 18 samples. The average activity concentration of  $^{137}\text{Cs}$  is 1.54 ± 0.13 Bqkg<sup>-1</sup>, and the range is 0.65-3.12 Bqkg<sup>-1</sup>. Associated radiological hazard indices including  $D$ ,  $AEDE$ ,  $ELCR$ ,  $H_{\text{ex}}$ ,  $H_{\text{in}}$ , and  $I_{\gamma}$  were also calculated. The values are lower than the safety

limits, which means no significant effect of the natural radiation exposure to the human health.

## ACKNOWLEDGMENT

This work was supported by Vietnam National Foundation for Science and Technology Development (NAFOSTED) under grant number 103.04-2021.131.

## AUTHORS' CONTRIBUTIONS

V. L. Bui and H. N. Tran designed and supervised the study, analyzed the data and wrote the manuscript. S. Leuangtakoun, L. Lathdavong and S. Xayhuangsy collected and prepared the soil samples. T. H. Bui, D. T. Duong and D. K. Tran performed the measurements and prepared the figures. V. K. Tran, N. T. Le, G. T. T. Phan and V. K. Hoang performed the data analysis.

## REFERENCES

- [1] \*\*\*, UNSCEAR, Radiation Sources and Effects of Ionizing Radiation, Report of the United Nations Scientific Committee on the Effect of Atomic Radiation to General Assembly, Technical Report, United Nations, New York, 2000
- [2] \*\*\*, UNSCEAR, Sources and Effects of Ionizing Radiation, Annex B: Exposures of the Public and Workers from Various Sources of Radiation, Technical Report, United Nations, New York, 2008
- [3] Singh, J., et al., Comparative Study of Natural Radioactivity Levels in Soil Samples from the Upper Siwaliks and Punjab, India Using Gamma-Ray Spectrometry, *Journal of Environmental Radioactivity*, 100 (2009), 1, pp. 94-98
- [4] Duong, V. H., et al., Characteristics of Radionuclides in Soil and Tea Plant (*Camellia Sinensis*) in Hoa Binh, Vietnam, *Journal of Radioanalytical and Nuclear Chemistry*, 329 (2021), 2, pp. 805-814
- [5] Rosas-Moreno, J., et al., Isolation and Identification of Arbuscular Mycorrhizal Fungi from an Abandoned Uranium Mine and Their Role in Soil-To-Plant Transfer of Radionuclides and Metals, *Science of the Total Environment*, 876 (2023), Mar., 162781
- [6] Uchida, S., et al., Uptake of Radionuclides and Stable Elements from Paddy Soil to Rice: A Review, *Journal of Environmental Radioactivity*, 100 (2009), 9, pp. 739-745
- [7] Semioshkina, N., Voigt, G., Soil – Plant Transfer of Radionuclides in Arid Environments, *Journal of Environmental Radioactivity*, 237 (2021), 1, 106692
- [8] Muthu, H., et al., Radioactivity Concentration and Transfer Factors of Natural Radionuclides  $^{226}\text{Ra}$ ,  $^{232}\text{Th}$ , and  $^{40}\text{K}$  from Peat Soil to Vegetables in Selangor, Malaysia, *Nucl Technol Radiat*, 37 (2022), 1, pp. 57-64
- [9] Al-Kharouf, et al., Natural Radioactivity, Dose Assessment and Uranium Uptake by Agricultural Crops at Khan Al-Zabeeb, Jordan, *Journal of Environmental Radioactivity*, 99 (2008), 7, pp. 1192-1199
- [10] Ribeiro, F. C. A., et al., Natural Radioactivity in Soils of the State of Rio de Janeiro (Brazil): Radiological Characterization and Relationships to Geological

- Formation, Soil Types and Soil Properties, *Journal of Environmental Radioactivity*, 182 (2018), Feb., pp. 34-43
- [11] Lee, S. K., et al., Radiological monitoring: terrestrial natural radionuclides in Kinta District, Perak, Malaysia, *Journal of Environmental Radioactivity*, 100 (2009), 5, pp. 368-374
- [12] Ahmad, N., et al., An Overview on Measurements of Natural Radioactivity in Malaysia, *Journal of Radiation Research and Applied Sciences*, 8 (2015), 1, pp. 136-141
- [13] Huy, N. Q., et al., Natural Radioactivity and External Dose Assessment of Surface Soils in Vietnam, *Radiation Protection Dosimetry*, 151 (2012), 3, pp. 522-531
- [14] Huy, N. Q., Luyen, T. V., Study on External Exposure Doses from Terrestrial Radioactivity in Southern Vietnam, *Radiation Protection Dosimetry*, 118 (2005), 3, pp. 331-336
- [15] Ngoc, B.V., et al., Study on the Characteristics of Natural Radionuclides in Surface Soil in Ho Chi Minh city, Vietnam and Radiological Health Hazard, *Environmental Earth Sciences*, 78 (2019), 1, 28
- [16] Tran, D. K., et al., Environmental Radioactivity and Associated Radiological Hazards in Surface Soils in Ho Chi Minh city, Vietnam, *Journal of Radioanalytical and Nuclear Chemistry*, 326 (2020), 3, pp. 1773-1783
- [17] Duong, N. T., et al., Natural Radionuclides and Assessment of Radiological Hazards in Muonghum, Lao Cai, Vietnam, *Chemosphere*, 270 (2021), 3, 128671
- [18] Alewell, C., et al., <sup>239+240</sup>Pu from Contaminant to Soil Erosion Tracer: Where do we stand? *Earth-Science Reviews*, 172 (2017), Aug., pp. 107-123
- [19] Meliho, M., et al., Assessment of Soil Erosion Rates in a Mediterranean Cultivated and Uncultivated Soils Using Fallout <sup>137</sup>Cs, *Journal of Environmental Radioactivity*, 208-209 (2019), 12, 106021
- [20] Meusburger, K., et al., A multi-Radionuclide Approach to Evaluate the Suitability of <sup>239+240</sup>Pu as Soil Erosion Tracer, *Science of The Total Environment*, 566-567 (2016), 1, pp. 1489-1499
- [21] Porto, P., Callegari, G., Using <sup>137</sup>Cs Measurements to Estimate Soil Erosion Rates in Forest Stands Affected by Wildfires, Results from Plot Experiments, *Applied Radiation and Isotopes*, 172 (2021), 12, 109668
- [22] Rogerio, d. A. F., et al., <sup>137</sup>Cs Activity Concentration in Soil of Alagoas State, Brazil, *Applied Radiation and Isotopes*, 170 (2021), Feb., 109607
- [23] Krstic, D., et al., Vertical Profile of <sup>137</sup>Cs in Soil, *Applied Radiation and Isotopes*, 61 (2004), 6, pp. 1487-1492
- [24] Hamzah, Z., et al., Assessment of <sup>137</sup>Cs Activity Concentration in Soil from Tea Plantation Areas in Cameron Highlands, *Journal of Nuclear and Related Technologies*, 9 (2012), 1, pp. 1-5
- [25] Xayheungsy, S., et al., Assessment of the Natural Radioactivity and Radiological Hazards in Lao Cement Samples, *Radiation Protection Dosimetry*, 181 (2018), 3, pp. 208-213
- [26] Bui, V. L., et al., Natural Radioactivity and Radiological Hazards in Soil Samples in Savannakhet Province, Laos, *Journal of Radioanalytical and Nuclear Chemistry*, 323 (2020), 1, pp. 303-315
- [27] Leuangtakoun, S., et al., Natural Radioactivity Measurement and Radiological Hazard Evaluation in Surface Soils in a Gold Mining Area and Surrounding Regions in Bolikhamxay province, Laos, *Journal of Radioanalytical and Nuclear Chemistry*, 326 (2020), 2, pp. 997-1007
- [28] Van, L. B., et al., Natural Radionuclides and Assessment of Radiological Hazards in Different Geological Formations in Khammouan Province, Laos, *Journal of Radioanalytical and Nuclear Chemistry*, 329 (2021), 2, pp. 991-1000
- [29] Nguyen, T. N., et al., Distribution and Characteristics of <sup>137</sup>Cs in Surface Soil in the Middle of Laos, *Journal of Radioanalytical and Nuclear Chemistry*, 332 (2023), 6, pp. 3661-3673
- [30] Ibrahim, N., Natural Activities of <sup>238</sup>U, <sup>232</sup>Th, and <sup>40</sup>K in Building Materials, *Journal of Environmental Radioactivity*, 43 (1999), 3, pp. 255-258
- [31] Loat, B., et al., The measurements of Uranium Enrichment by Using X-Rays and Gamma Rays Below 100 keV, *VNU Journal of Science: Mathematics – Physics*, 28 (2012), 2, pp. 77-83
- [32] Loat, B., et al., Experimental Determination of Enrichment of Uranium Material by Gamma-Spectroscopic Technique, *VNU Journal of Science: Mathematics – Physics*, 29 (2013), 2, pp. 33-39
- [33] Yucel, M. C., Demirel, H., Use of the 1001 keV Peak of <sup>234m</sup>Pa Daughter of <sup>238</sup>U in Measurement of Uranium Concentration by HPGE Gamma-Ray Spectrometry, Nuclear Instruments and Methods in Physics Research Section A: Accelerators, Spectrometers, Detectors and Associated Equipment, 413 (1998), 1, pp. 74-82
- [34] Loat, B. V., et al., Intrinsic Efficiency Calibration for Uranium Isotopic Analysis in Soil Samples, *VNU Journal of Science: Mathematics – Physics*, 33 (2017), 1, pp. 48-52
- [35] Krieger, R., Radioactivity of Construction Materials, *Betonwerk Fertigteile Technik*, 47 (1981), pp. 468-475
- [36] Beretka, J., Mathew, P. J., Natural Radioactivity of Australian Building Materials, Industrial Wastes and by-Products, *Health Physics*, 48 (1985), 1, pp. 87-95
- [37] Debertin, K., Helmer, R. G., *Gamma- and X-Ray Spectrometry with Semiconductor Detectors*, North-Holland, Amsterdam, Netherlands, 1988
- [38] Taskin, H., et al., Radionuclide Concentrations in Soil and Lifetime Cancer Risk Due to Gamma Radioactivity in Kirklareli, Turkey, *Journal of Environmental Radioactivity*, 100 (2009), 1, pp. 49-53
- [39] \*\*\*, ICRP, Compendium of Dose Coefficients Based on ICRP Publication 60, Technical Report, ICRP Publication 119. Ann. ICRP 41 (Suppl.), 2012
- [40] \*\*\*, UNSCEAR, Sources, Effects and Risks of Ionising Radiation, United Nations Scientific Committee on the Effects of Atomic Radiation, Technical Report, United Nations, New York, 1988
- [41] Kritsanuwat, R., et al., Natural Radioactivity Survey on Soils Originated from Southern Part of Thailand as Potential Sites for Nuclear Power Plants from Radiological Viewpoint and Risk Assessment, *Journal of Radioanalytical and Nuclear Chemistry*, 305 (2015), 2, pp. 487-499
- [42] Almayahi, B. A., et al., Effect of the Natural Radioactivity Concentrations and <sup>226</sup>Ra/<sup>238</sup>U Disequilibrium on Cancer Diseases in Penang, Malaysia, *Radiation Physics and Chemistry*, 81 (2012), 10, pp. 1547-1558
- [43] Saleh, M. A., et al., Assessment of <sup>226</sup>Ra Environmental <sup>232</sup>Th and <sup>40</sup>K, Concentrations in the Region of Elevated Radiation Background in Segamat District, Johor, Malaysia, *Journal of Environmental Radioactivity*, 124 (2013), May, pp. 130-140

Ди-Хонг БУИ<sup>1</sup>, Ван-Лоат БУИ<sup>1\*</sup>, Сомсавад ЛЕУАНГТАКУН<sup>2</sup>, Лемдонг ЛАТДАВОНГ<sup>2</sup>,  
Сонексај ХАЈХУАНГСИ<sup>2</sup>, Дук-Данг ДУОНГ<sup>3</sup>, Динх-Коа ТРАН<sup>4</sup>, Нгок-Диет ЛЕ<sup>1</sup>,  
Гианг Т. Т. ФАН<sup>5,6</sup>, Ван-Кан ХОАНГ<sup>7\*</sup>, Хоан-Нам ТРАН<sup>7\*</sup>

### КАРАКТЕРИСТИКЕ ПРИРОДНИХ РАДИОНУКЛИДА И $^{137}\text{Cs}$ У ПОВРШИНСКОМ ЗЕМЉИШТУ ФОНСАВАНА, У СЈЕНГКУАНГУ, ЛАОС

Процена карактеристика природних радионуклида и  $^{137}\text{Cs}$  у земљишту округа Фонсаван, у провинцији Сјенгкуанг, Лаос, спроведена је коришћењем стандардног електродног коаксијалног Ge (SEGe) детектора. Узорци земљишта прикупљени су на 20 локација у близини насељеног и пољопривредног подручја округа Фонсаван. Просечне концентрације активности  $^{226}\text{Ra}$ ,  $^{238}\text{U}$ ,  $^{232}\text{Th}$ ,  $^{40}\text{K}$  и  $^{137}\text{Cs}$  биле су  $54.0 \pm 2.5 \text{ Bqkg}^{-1}$ ,  $65.1 \pm 4.4 \text{ Bqkg}^{-1}$ ,  $96.9 \pm 3.7 \text{ Bqkg}^{-1}$ ,  $433.2 \pm 20.7 \text{ Bqkg}^{-1}$  и  $1.54 \pm 0.13 \text{ Bqkg}^{-1}$  респективно. Просечна активност еквивалента радијума  $Ra_{\text{eq}}$  била је  $175 \pm 20 \text{ Bqkg}^{-1}$ , а највиша вредност  $Ra_{\text{eq}}$  од  $269.9 \text{ Bqkg}^{-1}$  још увек је нижа од безбедносне границе од  $370 \text{ Bqkg}^{-1}$ . Придружени индекси радиолошке опасности, као што су јачина апсорбоване гама дозе, годишњи еквивалент ефективне дозе на отвореном, ризик од рака током живота, екстерни и унутрашњи индекси опасности и гама индекс, такође су израчунати и представљени.

*Кључне речи:* природни радионуклид,  $^{137}\text{Cs}$ , узорак земљишта, концентрација активности

---